Visualization and Analysis of Electroosmotic Flow in Hairless Mouse Skin

Bradley D. Bath,[1] Henry S. White,[1,3] and Erik R. Scott[2]

Received January 3, 2000; accepted January 24, 2000

Purpose. To identify the physiological structures in hairless mouse skin responsible for the generation of electroosmotic flow during iontophoresis. Also, to determine the effects of changing the pH of the contacting solution on the magnitude of electroosmotic flow in these structures.

Methods. Localized diffusive and iontophoretic fluxes of a neutral molecule, hydroquinone (HQ), across hairless mouse skin were quantified using scanning electrochemical microscopy (SECM). The iontophoretic flux was determined as a function of the direction of the applied current and pH of the contacting solution.

Results. SECM images of HQ transport recorded during iontophoresis at moderate current densities (± 0.1 mA/cm^2) demonstrate that electroosmotic flow is localized to hair follicles. The direction of flow is from anode to cathode at pH $>$ 3.5 and from cathode to anode at pH $<$3.5.

Conclusions. Electroosmotic flow through hair follicles is an efficient and controllable means of transporting small, electrically neutral molecules across hairless mouse skin. Transport through the appendages is sensitive to the pH of the solution in contact with the skin. The isoelectric point of hair follicles, pI, is estimated to be 3.5 from the dependence of electroosmotic flow on the solution pH.

KEY WORDS: scanning electrochemical microscopy; iontophoresis; hair follicle; electroosmotic flow; isoelectric point.

INTRODUCTION

New strategies for controlled-release drug delivery are being developed in response to difficulties associated with traditional methods of drug administration. Many drugs can not be administered orally due to extensive metabolism in the gastrointestinal tract or weak absorption into the bloodstream. Intravenous delivery avoids these problems, but is invasive and generally requires hospitalization. Advances during the past decade in transdermal drug delivery as an alternate to traditional methods of drug administration suggest that many drug molecules, including delicate peptides (1,2), proteins (3), and oligonucleotides (4–5) can be delivered across skin at a controlled rate and in an essentially non-invasive fashion. Iontophoretic transdermal drug delivery, which uses electrical currents to drive drug molecules across the skin, is a particularly attractive method since, in principle, the rate of delivery can be controlled with high precision by adjusting the electrical current (6). Iontophoretic transport of lidocaine and fentanyl is currently being employed for local and systemic anesthetic administration in clinical trials (6–7). Reverse iontophoretic transdermal transport, in which molecules in the blood stream are transported across the skin for analytical detection, is being developed for the noninvasive monitoring of blood glucose levels by diabetic patients (8).

In iontophoretic drug delivery, the molecule of interest is contained in a solution that is in contact with the outer layer of skin, the stratum corneum. An electrical current, typically a few hundred microamperes per square centimeter, is passed through the solution, driving charged molecules by electrical migration into the underlying dermal tissue. A number of experimental studies, based on staining of pores during iontophoresis of charged dyes, as well as using scanning microelectrode techniques, have shown that skin appendages (e.g., hair follicles and sweat glands) are associated with regions of high electrical current density (9–12). For instance, scanning electrochemical microscopy (SECM), combined with dye staining techniques, has been used to quantitatively demonstrate that iontophoretic current across hairless mouse skin is predominantly transported through hair follicles (13).

Recent studies have demonstrated that the electrical current can also enhance the rate of transport of electrically neutral molecules (6,14–18). This result suggests that iontophoresis induces an electroosmotic flow of solution across skin tissues (14). Transport of a drug molecule by electroosmosis requires that the epidermal layers contain a porous permselective phase. To our knowledge, no physiological structure in skin has been directly associated with this type of flow. Herein we report direct observations of electroosmotic flows in hairless mouse skin during iontophoresis at moderate applied current densities (± 0.1 mA/cm^2) and at different solution pH's. Specifically, our experiments demonstrate that electroosmotic flow is localized to hair follicles in hairless mouse skin and that varying the pH of the solution contacting the epidermal and dermal tissues can control the direction and magnitude of flow. The results suggest that the permselective characteristics of skin that are responsible for electroosmotic flow are associated with the epithelial cell layers that define the hair follicles (19).

MATERIALS AND METHODS

Chemicals

Hydroquinone was obtained from Aldrich Chemical Company and was used as received. Diluted hydrochloric acid (Mallinckrodt) was used to adjust the pH of the contacting solutions. All solutions were prepared using deionized water (resistivity $= 18$ mΩ cm) obtained from a Barnstead E-Pure™ water purification system.

Skin

The skin was excised from 7 week-old male hairless mice (Charles River SKH-1) immediately after euthanasia by CO_2 asphyxiation. The excised skin was stored in phosphate buffered saline (Dulbecco's, D-PBS) saturated gauze pads. The tissue was then kept under refrigeration and used within 24 hours of sacrifice. The research adhered to the "Principles of Laboratory Animal Care" (NIH publication #85-23, revised 1985).

[1] Department of Chemistry, University of Utah, Salt Lake City, Utah 84112.

[2] ALZA Corporation, Spring Lake Park, Minnesota 55432.

[3] To whom correspondence should be addressed. (e-mail: white@chemistry.utah.edu)

0724-8741/00/0400-0471$18.00/0

Scanning Electrochemical Microscopy

In the present report, scanning electrochemical microscopy (SECM) (20) is used to image and quantify the rate of electroosmotic transport across hairless mouse skin (HMS). A detailed description of the microscope and methodology for imaging porous membranes has been previously reported (20,21). Figure 1 shows the iontophoresis cell and key components of the microscope. A sample of full-thickness HMS is placed in the diffusion cell (21), separating the donor (lower) and receptor (upper) solutions. In the present studies, a neutral electrochemically active permeant, hydroquinone (HQ), is dissolved in the donor solution and is allowed to diffuse across the skin sample to the receptor solution. HQ is a weak acid with $pK_a = 10.4$ (22); all investigations were performed at pH below 7, ensuring that HQ exists in its protonated and electrically neutral form. To study iontophoretic transport, a constant electrical current, i_{app}, is applied between the two Ag/AgCl electrodes that are positioned on opposite sides of the HMS sample (Fig. 1). HQ is electrochemically detected at the SECM tip through the redox reaction, eq. (1),

$$HQ \rightleftharpoons BQ + 2H^+ + 2e^- \qquad E^{\circ\prime} = 0.477V \text{ vs Ag/AgCl} \qquad (1)$$

as it emerges from the skin into the receptor solution. In Eq. (1), BQ is the product species, benzoquinone, and $E^{\circ\prime}$ is the reversible potential of the HQ/BQ redox couple (). The SECM tip is an electrochemically etched Pt wire insulated by a thin layer of polyphenylene oxide except at the very tip of the wire (20). The radius of the exposed tip varies between 0.5–5.0 μm. The tip position is controlled using three piezoelectric (*x, y, z*) inchworm motors, as previously described (20,21). A video camera with 100× magnification is used to observe the tip above the skin surface. The height of the tip is determined by lowering the tip until it touches the skin surface, then retracting it using the *z*-inchworm motor. Because skin has a fairly rough surface, the height of the tip is known only to within ±2 μm.

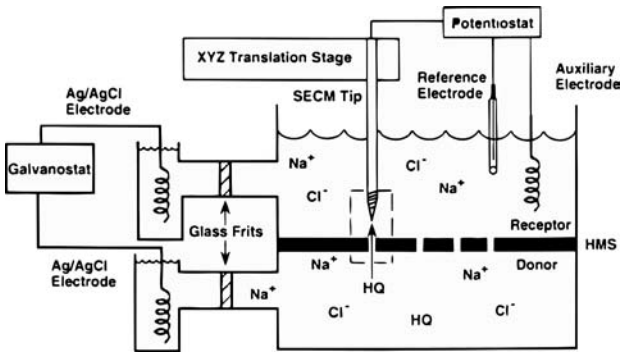

Fig. 1. Schematic diagram of the scanning electrochemical microscope (SECM) and iontophoresis cell used for imaging the molecular flux of HQ across hairless mouse skin. The two large Ag/AgCl electrodes and galvanostat are used to apply iontophoretic current (i_{app}). The skin separates a donor solution containing supporting electrolyte (0.2 M NaCl) and the electroactive molecular permeant (0.2 M HQ) from a receptor solution containing only supporting electrolyte. The SECM tip is rastered above the strateum corneum surface at a fixed height (~20 μm) and is used to electrochemically detect HQ as it enters the receptor compartment.

RESULTS AND DISCUSSION

SECM Measurement of Localized Molecular Flux

Fig. 2a depicts the SECM tip positioned above a HMS sample. Typically, in the experiments reported herein, the tip is positioned ~20 μm above the stratum corneum surface. Fig. 2b shows the steady-state voltammetric response of the tip when it is positioned directly above a hair follicle opening (curve 1) and at a lateral distance of ~150 μm from the opening (curve 2). Both responses are obtained without applying a current across the skin (i.e., $i_{app} = 0$). The sigmoidal shaped voltammetric wave recorded above the hair follicle (curve 1) corresponds to oxidation of HQ molecules that have diffused across the skin sample through the hair follicle. The magnitude of the tip voltammetric current is proportional to the local rate at which HQ permeates the skin (20). The SECM tip current decreases to background levels (curve 2) when the tip is moved away from the pore opening, demonstrating that the diffusive flux of HQ is localized to the hair follicle. The sites of high diffusive flux are identified as hair follicles using a dye staining technique in which colloidal prussian blue is precipitated at the opening of the follicle (13,23).

SECM images presented in Fig. 3 demonstrate that electroosmotic transport of HQ is operative inside the hair follicle

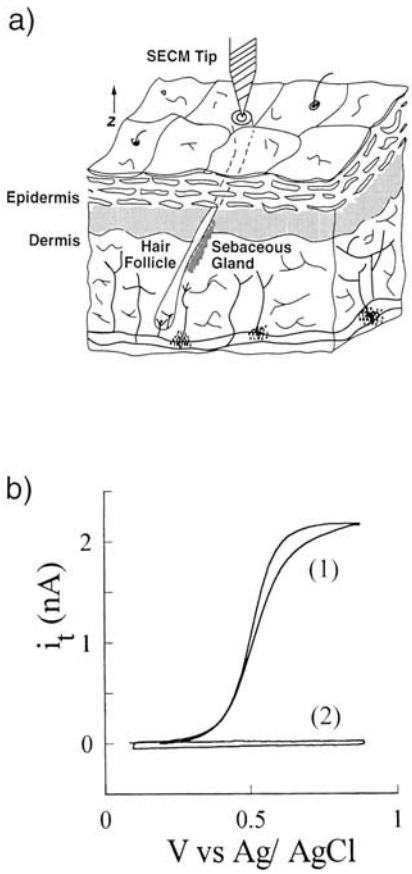

Fig. 2. (a) Schematic drawing illustrating the SECM tip positioned directly above the opening of a hair follicle. (b) Voltammetric response of a 2.7 μm-radius SECM tip positioned directly above a hair follicle opening (curve 1) and 150 μm away from the opening (curve 2). The voltammetric current corresponds to oxidation of HQ (eq. (1)) that has diffused through the hair follicle.

(in addition to diffusion) when a constant iontophoretic current, i_{app}, is applied across the skin sample. The donor and receptor solutions were maintained at pH = 6.0 in this set of experiments. The SECM images were recorded by rastering the SECM tip at a fixed height (~20 μm) above the opening of a hair follicle while biasing the tip potential at 0.9 V vs. Ag/AgCl in order to detect HQ. The middle image was obtained at $i_{app} = 0$, corresponding to diffusion of HQ. The bottom image, obtained at $i_{app} = 50$ μA, clearly demonstrates that a positive iontophoretic current enhances the rate of molecular transport through the hair follicle. Because HQ is electrically neutral at pH = 6.0, its transport is not directly influenced by the applied current. Rather, the enhancement in molecular transport must result from electroosmotic flow of solution inside the hair follicle.

In our experiments, the application of a positive i_{app} corresponds to the upward migration of electrolyte cations (Na^+) from the donor to the receptor solution and/or the downward migration of anions (Cl^-), i.e., the anode is in the donor compartment. The direction of electroosmotic flow that is induced by the current depends upon the permselective properties of the skin sample. HMS, which exhibits a net negative charge at pH = 6.0 (24,25), displays cation-selective membrane properties (24) (the transference number for Na^+ in HMS is twice as large as that for Cl^- (30)). Thus, the majority charge carrier in skin at pH = 6.0 is Na^+. The cation permselectivity of HMS may arise from protein chemistry similar to that of human skin; it is reported that the observed permselectivity results from a larger number of carboxylate ($-COO^-$) than ammonium ($-NH_3^+$) groups (associated with protein amino acid residues) that reside in epidermal and dermal tissues (26). The increase in HQ flux at positive i_{app} (Fig. 3) is consistent with the reported cation-selectivity of HMS. Na^+ transport and electroosmotic flow at positive i_{app} are in the same direction as diffusion of HQ, thus enhancing the transport of the molecule relative to diffusion alone.

When the direction of the current is reversed, i.e., when i_{app} is negative and the anode is in the receptor compartment, the directions of Na^+ migration and electroosmotic flow are also reversed. In this case, electroosmotic flow should oppose the diffusion of HQ through the hair follicle, resulting in a decrease in the total flux of HQ. SECM images recorded at negative i_{app} (top image, Fig. 3) show that the HQ transport rate is indeed reduced when electroosmotic flow opposes the diffusion of HQ.

As noted above, the direction of electroosmotic flow is determined in part by the acid-base properties of the epidermal and dermal tissues. The isoelectric point, pI, of skin, i.e., the pH at which skin is electrically neutral, is estimated by Pikal and Shah to be slightly below 3.8 (25) and has been measured to be between 4.5 and 4.6 by Luzardo-Alverez et al. (27). HMS is negatively charged at pH's above the pI and, thus, exhibits cation permselectivity at pH = 6.0, as demonstrated by the transport studies described above. At pH's below the pI, skin is expected to have a net positive electrical charge, and should exhibit anion permselectivity. Thus, assuming that the pI of the epithelial cells lining the hair follicle is between 3.8 and 4.5, it should be possible to reverse the direction of electroosmotic flow by lowering the pH of the contacting solutions from a value above the pI to a value below the pI.

Fig. 4 shows the results of iontophoretic experiments performed at pH's above, below, and near the pI of HMS. The SECM tip was positioned above a hair follicle to voltammetrically detect HQ as a function of i_{app}. At pH = 6.0, Na^+ is the predominant current carrier, and the application of a positive i_{app} results in an enhanced HQ flux due to electroosmotic flow of solution from the donor to the receptor solution (analogous to the results in Fig. 3). At pH = 3.5, which corresponds

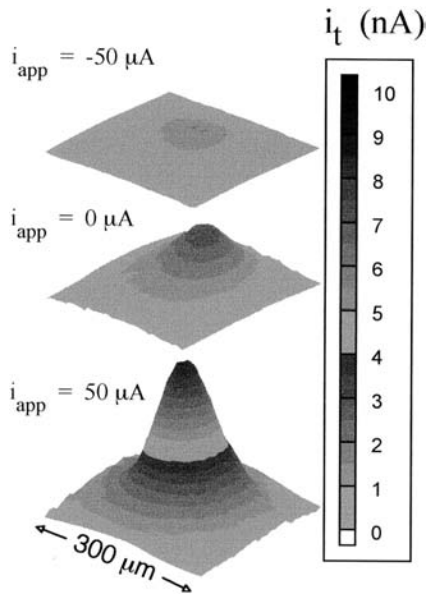

Fig. 3. SECM images of HQ emerging from the opening of a hair follicle as a function of the applied iontophoretic current at pH = 6.0. The center image corresponds to diffusion of HQ from the donor to the receptor solution. The lower image corresponds to positive current ($i_{app} = 50$ μA), inducing electroosmotic flow in the same direction as diffusion. The upper image corresponds to a negative current ($i_{app} = -50$ μA), resulting in electroosmotic flow opposing diffusion. A 2.6 μm-radius SECM tip, biased at 0.9 V vs. Ag/AgCl, was used to record the images.

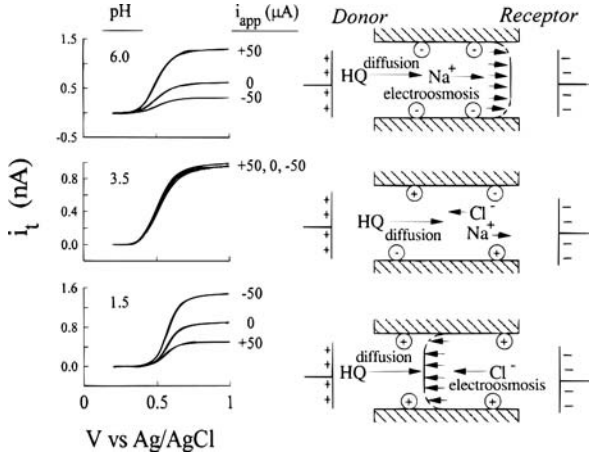

Fig. 4. Electroosmotic flow as a function of the pH of the donor and receptor solutions. The SECM tip is positioned directly above a hair follicle and the voltammetric response is recorded as a function of iontophoretic current (i_{app}) and pH. At pH = 3.5 (middle), the iontophoretic current has a negligible effect on the transport of HQ indicating that electroosmotic flow does not occur at this pH. The schematic diagrams show the relative directions of HQ diffusion, ion transport, and electroosmotic flow at $i_{app} = 50$ μA.

approximately to the isoelectric point of a hair follicle (see discussion below), the application of an electrical current has no significant effect on the rate of transport of HQ in the hair follicle. Thus, at this pH, Na^+ and Cl^- carry approximately the same fraction of the current and electroosmotic flow is not operative. At pH = 1.5, the application of a positive i_{app} is observed to cause a decrease in the transport of HQ. This is consistent with skin bearing a net positive charge at pH's below the pI of HMS. The dependence of the direction of the electroosmotic flux on pH is reversible. Increasing the pH from 1.5 back to 6.0 results in an enhancement in HQ flux at positive i_{app} (data not shown), indicating that the observed dependence of electroosmotic flow on pH is not a result of damage to the skin in the acidic solutions (25).

The dependence of electroosmotic flow on pH may be quantified using the enhancement factor, *E*, which is defined as the ratio of the fluxes of HQ under iontophoretic (N_{iont}) and diffusive (N_{diff}) conditions, i.e., $E = N_{iont}/N_{diff}$. Because the SECM tip current above a hair follicle is proportional to the local flux (20), values of *E* can be readily determined from the ratio of the voltammetric currents measured under iontophoretic and diffusive conditions. Fig. 5 shows *E* as a function of pH for $i_{app} = -50$ and 50 μA. The data correspond to average values of measurements on two hair follicles located on different skin sections. Fig. 5 demonstrates that *E* is equal to unity at pH ~ 3.5, indicating that electroosmotic flow is not operative near the reported pI of HMS. This finding, in addition to the sigmoidal shape of the *E* vs. pH curves, suggests that the direction and magnitude of electroosmotic flow in the hair follicle is determined by the acid-base equilibria of the protein amino acid residues located in the epithelial cells comprising the hair follicle structure.

Analysis of Electroosmotic Flow in Hair Follicles

The relationship between *E* and the electroosmotic velocity, v_{eo}, is obtained from the expression for the diffusive-convective flux, N_{iont}, of a neutral molecule (20):

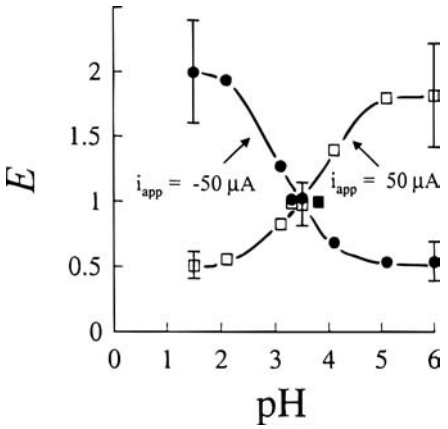

Fig. 5. Flux enhancement factor, *E*, at positive and negative iontophoretic currents as a function of pH. *E* is equal to unity at pH ~ 3.5, corresponding to the pI of the epithelial cell layers comprising the hair follicle structure. The donor solution contains 0.2 M HQ and 0.2 M NaCl; the receptor solution contains 0.2 M NaCl. The pH of the solutions were adjusted by addition of hydrochloric acid. Error bars for data at pH = 1.5, 3.5, and 6.0 represent one standard deviation and are computed based on five replicate measurements (Table I). The remaining data points represent the average of two measurements.

$$N_{iont} = -D_{hf}\frac{\partial C_{hf}}{\partial z} + v_{eo}C_{hf}. \quad (2)$$

In eq. (2), C_{hf} and D_{hf} are the local concentration and diffusivity, respectively, of HQ in the hair follicle. In the absence of an applied iontophoretic current, the diffusive flux of HQ is given by $N_{diff} = -D_{hf}(\partial C_{hf}/\partial z)$. Following the procedure described in ref. (28), integration of the expressions for N_{iont} and N_{diff} over the length of a hair follicle, ℓ, yields *E* in terms of v_{eo}.

$$E = N_{iont}/N_{diff} = (v_{eo}\ell/D_{hf})/\{1 - \exp(-v_{eo}\ell/D_{hf})\} \quad (3)$$

If ℓ and D_{hf} are known, then the experimental value of *E* can be used to estimate the electroosmotic velocity of HQ in the hair follicle (eq. (3)).

The thickness of HMS has been measured to be ~500 μm (29). In order to estimate ℓ, we assume that HQ enters the interior of the hair follicle by traversing the epithelial cell layers that line the hair follicle between the bulb and the dermis/epidermis boundary (Fig. 2a). Because HQ most likely enters into the hair follicle throughout this range, we use an average value of $\ell \sim 300$ μm. We assume that diffusion of HQ in the bulk dermis is relatively rapid and that molecular transport is limited by convective-diffusion once the molecule has entered the narrow hair follicle. A value of D_{hf} is estimated from the temporal response of an SECM tip above a hair follicle in response to a step increase or decrease in i_{app}. The time required to obtain a steady flux of HQ in a hair follicle (t) was measured and used to compute D_{hf} from the relation, $\ell^2 = 6D_{hf}t$ (30). We find that $D_{hf} \approx 0.83 \times 10^{-6}$ cm²/s, approximately one order of magnitude smaller than the diffusivity of HQ in bulk aqueous solution (20).

Table I summarizes values of *E* and the corresponding values of v_{eo} as a function of pH. At pH = 6.0 and $i_{app} = 50$

Table I. Iontophoretic Enhancements and Electroosmotic Velocities as a Function of pH

pH	Hair follicle[a]	*E* (50 μA)	*E* (−50 μA)
6.0	1	1.4	0.86
	2	1.9	0.44
	3	2.5	0.49
	4	2.1	0.64
	5	1.9	0.62
		2.0 ± 0.4	0.61 ± 0.2
		v_{eo} = 0.42 (± 0.15) μm/s	− 0.26 (± 0.13) μm/s
3.5	1	0.81	1.2
	2	0.92	1.0
	3	0.99	1.1
	4	1.0	1.0
	5	0.97	1.1
		0.94 ± 0.08	1.1 ± 0.1
		v_{eo} = −0.037 (± 0.049) μm/s	0.043 (± 0.040) μm/s
1.5	1	0.65	1.4
	2	0.63	1.8
	3	0.45	2.3
	4	0.44	2.8
	5	0.48	2.1
		0.53 ± 0.10	2.1 ± 0.5
		v_{eo} = −0.33 (± 0.09) μm/s	0.46 (± 0.19) μm/s

[a] One hair follicle per skin section was analyzed. Each skin section was taken from a different animal.

μA, electroosmotic flow enhances the diffusional flux of HQ by a factor of 2. 0 ± 0.4. Using this value, we compute (eq. (3)) an electroosmotic velocity of 0.42 ± 0.15 μm/s (the positive sign indicates flow occurs in the same direction as HQ diffusion, from the donor to receptor solution). Reversing the current ($i_{app} = -50$ μA), results in an enhancement factor less that unity, $E = 0.61 \pm 0.2$, corresponding to an electroosmotic flow velocity of -0.26 ± 0.13 μm/s. The results indicate that electroosmotic flow in hair follicles occurs in both directions, albeit slightly slower when flow is directed from the epidermal to dermal side. The data in Table I also illustrate that the electroosmotic flow occurs at the same velocity, but in opposite directions, at pH = 6.0 and 1.5, illustrating the pH-dependent permselectivity of HMS.

The SECM images and analysis reported above demonstrate that electroosmotic flows in HMS are localized to hair follicles. It is most likely that these flows originate in the (pH-dependent) charged epithelial cell layers comprising the structure of the hair follicle. The electroosmotic flow generated in the cell layers "pumps" solution along the length of the hair follicle. To our knowledge these are the first quantitative measurements that directly identify physiological structures associated with electroosmotic transport in skin. Preliminary SECM measurements in our laboratory indicate that electroosmotic transport of hydroquinone is also localized to appendages in human cadaver skin.

Our results demonstrate that hair follicles in HMS provide an efficient and controllable pathway for delivery of small molecules into the body at moderate current densities. Advances in the fundamental understanding of iontophoretic transport across skin may assist in the future design and engineering of controlled-release and diagnostic devices. For instance, the time required for a molecule to traverse HMS tissues by electroosmotic flow can be estimated from $t_{eo} = \ell/v_{eo}$. Using $\ell \approx 300$ μm and the value of v_{eo} in a single hair follicle at $i_{app} = 50$ μA (0.42 μm/s, Table I) yields $t_{eo} \sim 12$ minutes. This value represents the minimum time for transdermal delivery of an electrically neutral molecule across HMS by electroosmotic transport.

ACKNOWLEDGMENTS

This work was funded by ALZA Corporation. We would like to thank Prof. William I. Higuchi (University of Utah) for many helpful discussions and insight into the project.

REFERENCES

1. L. L. Miller, C. J. Kolaskie, G. A. Smith, and J. Rivier. Transdermal iontophoresis of gonadotropin releasing hormone and two analogues. *J. Pharm. Sci.* **79**:490–493 (1990).
2. K. S. Bhatia and J. Singh. Mechanism of transport enhancement of LHRH through porcine epidermis by terpenes and iontophoresis: permeability and lipid extraction studies. *Pharm. Res.* **15**:1857–1862 (1998).
3. S. Mitragotri, D. Blankschtein, and R. Langer. Ultrasound-mediated transdermal protein delivery. *Science* **269**:850–853 (1995).
4. R. H. Brand, A. Wahl, and P. L. Iversen. Effects of size and sequence on the iontophoretic delivery of oligonucleotides. *J. Pharm. Sci.* **87**:49–52 (1998).
5. K. Oldenburg, K. T. Vo, G. A. Smith, and H. E. Selick. Iontophoretic delivery of oligonucleotides across full thickness hairless mouse skin. *J. Pharm. Sci.* **84**:915–921 (1995).
6. A. K. Banga. *Electrically Assisted Transdermal and Topical Drug Delivery*, Taylor and Francis, Pennsylvania, 1998.
7. S. K. Gupta, M. Southam, G. Sathyan, and M. Klausner. Effect of current density on pharmacokinetics following continuous or intermittent input from a fentanyl electrotransport system. *J. Pharm. Sci.* **87**:976–981 (1998).
8. J. A. Tamada, N. J. V. Bohannon, and R. O. Potts. Measurement of glucose in diabetic subjects using non-invasive transdermal extraction. *Nature Med.* **1**:1198–1201 (1995).
9. H. A. Abramson and M. G. Engle. Skin reactions. XII. Patterns produced in the skin by electrophoresis of dyes. *Arch. Dermatol. Syphilol.* **44**:190–200 (1941).
10. S. Grimmes. Pathways of ionic flow through human skin in vivo. *Acta Derm. Venereol.* **64**:93–98 (1984).
11. R. R. Burnette and B. Ongpipattanakul. Characterization of the pore transport properties and tissue alteration of excised human skin during iontophoresis. *J. Pharm. Sci.* **77**:132–137 (1988).
12. C. Cullander and R. H. Guy. Sites of iontophoretic current flow into the skin: Identification and characterization with the vibrating probe electrode. *J. Invest. Dermatol.* **97**:55–64 (1991).
13. E. R. Scott, A. I. Laplaza, H. S. White, and J. B. Phipps. Transport of ionic species in skin: contribution of pores to the overall skin conductance. *Pharm. Res.* **10**:1699–1709 (1993).
14. M. J. Pikal. The role of electroosmosis in transdermal iontophoresis. *Adv. Drug Del. Rev.* **9**:201–237 (1992).
15. M. B. Delgado-Charro and R. H. Guy. Characterization of convective solvent flow during iontophoresis. *Pharm. Res.* **11**:929–935 (1994).
16. K. D. Peck, V. Srinivasan, S. K. Li, W. I. Higuchi, and A. H. Ghanem. Quantitative description of the effect of molecular size upon electroosmotic flux enhancement during iontophoresis for a synthetic membrane and human epidermal membrane. *J. Pharm. Sci.* **85**:781–788 (1996).
17. R. Y. Lin, Y. C. Chien, and W. Y. Chen. The role of electroosmotic flow on *in vitro* transdermal iontophoresis. *J. Contr. Rel.* **43**: 23–33 (1997).
18. S. M. Sims and W. I. Higuchi. Baseline studies on iontophoretic transport in hairless mouse skin: the effect of applied voltage drop and pH on the iontophoresis of a model weak electrolyte. *J. Membr. Sci.* **49**:305–320 (1990).
19. G. F. Odland. Structure of the Skin. In L. A. Goldsmith (ed.). *Biochemistry and Physiology of the Skin*, Oxford University Press, Oxford, 1983.
20. B. D. Bath, R. D. Lee, H. S. White, and E. R. Scott. Imaging molecular transport in porous membranes. Observation and analysis of electroosmotic flow in individual pores using the scanning electrochemical microscope. *Anal. Chem.* **70**:1047–1058 (1998).
21. E. R. Scott, H. S. White, and J. B. Phipps. Iontophoretic transport through porous membranes using scanning electrochemical microscopy: application to *in vitro* studies of ion fluxes through skin. *Anal. Chem.* **65**:1537–1545 (1993).
22. R. C. Weast and M. J. Astle (eds.). *Handbook of Chemistry and Physics*, CRC Press, Boca Raton, 1981.
23. R. D. Lee, H. S. White, E. R. Scott. Visualization of iontophoretic transport paths in cultured and animal skin models. *J. Pharm. Sci.* **85**:1186–1190 (1996).
24. R. R. Burnette and D. Marrero. Comparison between the iontophoretic and passive transport of thyrotropin releasing hormone across excised nude mouse skin. *J. Pharm. Sci.* **75**:738–743 (1986).
25. M. J. Pikal and S. Shah. Transport mechanisms in iontophoresis. II. Electroosmotic flow and transference number measurements for hairless mouse skin. *Pharm. Res.* **7**:213–221 (1990).
26. R. R. Burnette and B. Ongpipattanakul. Characterization of the permselective properties of excised human skin during iontophoresis. *J. Pharm. Sci.* **76**:765–773 (1987).
27. A. Luzardo-Alverez, M. Rodríguez-Fernández, J. Blanco-Méndez, R. H. Guy, and M. B. Delgado-Charro. Iontophoretic permselectivity of mammalian skin: Characterization of hairless mouse and porcine membrane models. *Pharm. Res.* **15**:984–987 (1998).
28. V. Srinivasan and W. I. Higuchi. A model for iontophoresis incorporating the effect of convective solvent flow. *Int. J. Pharm.*, **60**:133–137 (1990).
29. R. L. Bronaugh, R. F. Stewart, and E. R. Congdon. Methods for *in vitro* percutaneous absorption studies. II. Animal models for human skin. *Toxicol. Appl. Pharmacol.* **62**:481–489 (1982).
30. J. Crank, *The Mathematics of Diffusion, 2nd Edition*, Oxford Science Publications, Oxford, 1975, page 50.